Supplementary Material – Multi-Stage Progressive Image Restoration

Syed Waqas Zamir*[1] Aditya Arora*[1] Salman Khan[2] Munawar Hayat[3]
Fahad Shahbaz Khan[2] Ming-Hsuan Yang[4,5,6] Ling Shao[1,2]
[1]Inception Institute of AI [2]Mohamed bin Zayed University of AI [3]Monash University
[4]University of California, Merced [5]Yonsei University [6]Google Research

1. Additional Ablation on ORSNet design

In the last stage of the proposed architecture, we employ the original-resolution subnetwork (ORSNet). Table 1 shows the impact of changing the original-resolution blocks (ORBs) and channel-attention blocks (CABs). While increasing the number of ORBs and CABs in ORSNet consistently improves accuracy, we use 3 ORBs and 8 CABs so to have a good trade-off between speed and accuracy.

2. Detailed Diagram of CSFF

Cross-stage feature fusion (pink arrows in Fig. 2 of the main paper) is shown at one level for brevity. However, this process is repeated at each level of the encoder-decoder, as shown in Fig 1.

3. Training Times

On two NVIDIA Tesla V100 GPUs, our MPRNet takes training time of approximately 37 hours for deraining, 62 hours for denoising, and 86 hours for deblurring.

4. Image Deraining Results

Figures 2, 3 and 4 show deraining results of our MPRNet and those of the state-of-the-art on several challenging images from different datasets. Our method effectively removes rain streaks and yields good quality images both visually and in terms of PSNR.

5. Image Deblurring Results

Here we test the performance of different image deblurring methods on synthetic as well as real datasets. For the case of synthetic datasets, the visual results are shown in Figures 5 and 6 on the GoPro dataset [7], and in Figures 7 and 8 on the HIDE dataset [12]. We further evaluate the competing methods on real-world images of the RealBlur dataset [11] and results are presented in Figures 9 and 10 for the RealBlur-J subset and in Figures 11 and 12 for the RealBlur-R subset.

*Equal contribution

Table 1: Ablation: the impact of increasing ORBs and CABs in the ORSNet subnetwork.

#ORBs	#CABs	PSNR
3	4	28.39
2	8	28.70
3	8	28.96
4	8	29.07
4	10	29.10

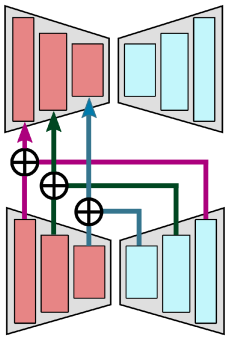

Figure 1: Cross-stage feature fusion between the encoder-decoders of stage 1 and stage 2.

6. Image Denoising Results

We provide additional denoising comparisons of our method with the state-of-the-art. Results on the SIDD dataset [1] are shown in Figures 13 and 14. And visual examples on the DND dataset [9] are illustrated in Figure 15.

References

[1] Abdelrahman Abdelhamed, Stephen Lin, and Michael S Brown. A high-quality denoising dataset for smartphone cameras. In *CVPR*, 2018. 1, 14, 15

[2] Meng Chang, Qi Li, Huajun Feng, and Zhihai Xu. Spatial-adaptive network for single image denoising. In *ECCV*, 2020. 14, 15, 16

[3] Kui Jiang, Zhongyuan Wang, Peng Yi, Baojin Huang, Yimin Luo, Jiayi Ma, and Junjun Jiang. Multi-scale progressive

fusion network for single image deraining. In *CVPR*, 2020. 3, 4, 5

[4] Yoonsik Kim, Jae Woong Soh, Gu Yong Park, and Nam Ik Cho. Transfer learning from synthetic to real-noise denoising with adaptive instance normalization. In *CVPR*, 2020. 14, 15, 16

[5] Orest Kupyn, Tetiana Martyniuk, Junru Wu, and Zhangyang Wang. DeblurGAN-v2: Deblurring (orders-of-magnitude) faster and better. In *ICCV*, 2019. 6, 7, 8, 9, 10, 11, 12, 13

[6] Xia Li, Jianlong Wu, Zhouchen Lin, Hong Liu, and Hongbin Zha. Recurrent squeeze-and-excitation context aggregation net for single image deraining. In *ECCV*, 2018. 3, 4, 5

[7] Seungjun Nah, Tae Hyun Kim, and Kyoung Mu Lee. Deep multi-scale convolutional neural network for dynamic scene deblurring. In *CVPR*, 2017. 1, 6, 7

[8] Dongwon Park, Dong Un Kang, Jisoo Kim, and Se Young Chun. Multi-temporal recurrent neural networks for progressive non-uniform single image deblurring with incremental temporal training. In *ECCV*, 2020. 6, 7, 8, 9

[9] Tobias Plotz and Stefan Roth. Benchmarking denoising algorithms with real photographs. In *CVPR*, 2017. 1, 16

[10] Dongwei Ren, Wangmeng Zuo, Qinghua Hu, Pengfei Zhu, and Deyu Meng. Progressive image deraining networks: A better and simpler baseline. In *CVPR*, 2019. 3, 4, 5

[11] Jaesung Rim, Haeyun Lee, Jucheol Won, and Sunghyun Cho. Real-world blur dataset for learning and benchmarking deblurring algorithms. In *ECCV*, 2020. 1, 10, 11, 12, 13

[12] Ziyi Shen, Wenguan Wang, Xiankai Lu, Jianbing Shen, Haibin Ling, Tingfa Xu, and Ling Shao. Human-aware motion deblurring. In *ICCV*, 2019. 1, 8, 9

[13] Maitreya Suin, Kuldeep Purohit, and A. N. Rajagopalan. Spatially-attentive patch-hierarchical network for adaptive motion deblurring. In *CVPR*, 2020. 6, 7, 8, 9

[14] Xin Tao, Hongyun Gao, Xiaoyong Shen, Jue Wang, and Jiaya Jia. Scale-recurrent network for deep image deblurring. In *CVPR*, 2018. 6, 7, 8, 9, 10, 11, 12, 13

[15] Wei Wei, Deyu Meng, Qian Zhao, Zongben Xu, and Ying Wu. Semi-supervised transfer learning for image rain removal. In *CVPR*, 2019. 3, 4, 5

[16] Wenhan Yang, Robby T Tan, Jiashi Feng, Jiaying Liu, Zongming Guo, and Shuicheng Yan. Deep joint rain detection and removal from a single image. In *CVPR*, 2017. 4, 5

[17] Rajeev Yasarla and Vishal M Patel. Uncertainty guided multi-scale residual learning-using a cycle spinning cnn for single image de-raining. In *CVPR*, 2019. 3, 4, 5

[18] Zongsheng Yue, Qian Zhao, Lei Zhang, and Deyu Meng. Dual adversarial network: Toward real-world noise removal and noise generation. In *ECCV*, 2020. 14, 15, 16

[19] Syed Waqas Zamir, Aditya Arora, Salman Khan, Munawar Hayat, Fahad Shahbaz Khan, Ming-Hsuan Yang, and Ling Shao. CycleISP: Real image restoration via improved data synthesis. In *CVPR*, 2020. 14, 15, 16

[20] Hongguang Zhang, Yuchao Dai, Hongdong Li, and Piotr Koniusz. Deep stacked hierarchical multi-patch network for image deblurring. In *CVPR*, 2019. 6, 7, 8, 9, 10, 11, 12, 13

[21] He Zhang and Vishal M Patel. Density-aware single image de-raining using a multi-stream dense network. In *CVPR*, 2018. 3, 4

[22] He Zhang, Vishwanath Sindagi, and Vishal M Patel. Image de-raining using a conditional generative adversarial network. *TCSVT*, 2019. 3, 5

[23] Kaihao Zhang, Wenhan Luo, Yiran Zhong, Lin Ma, Bjorn Stenger, Wei Liu, and Hongdong Li. Deblurring by realistic blurring. In *CVPR*, 2020. 6, 7, 8, 9

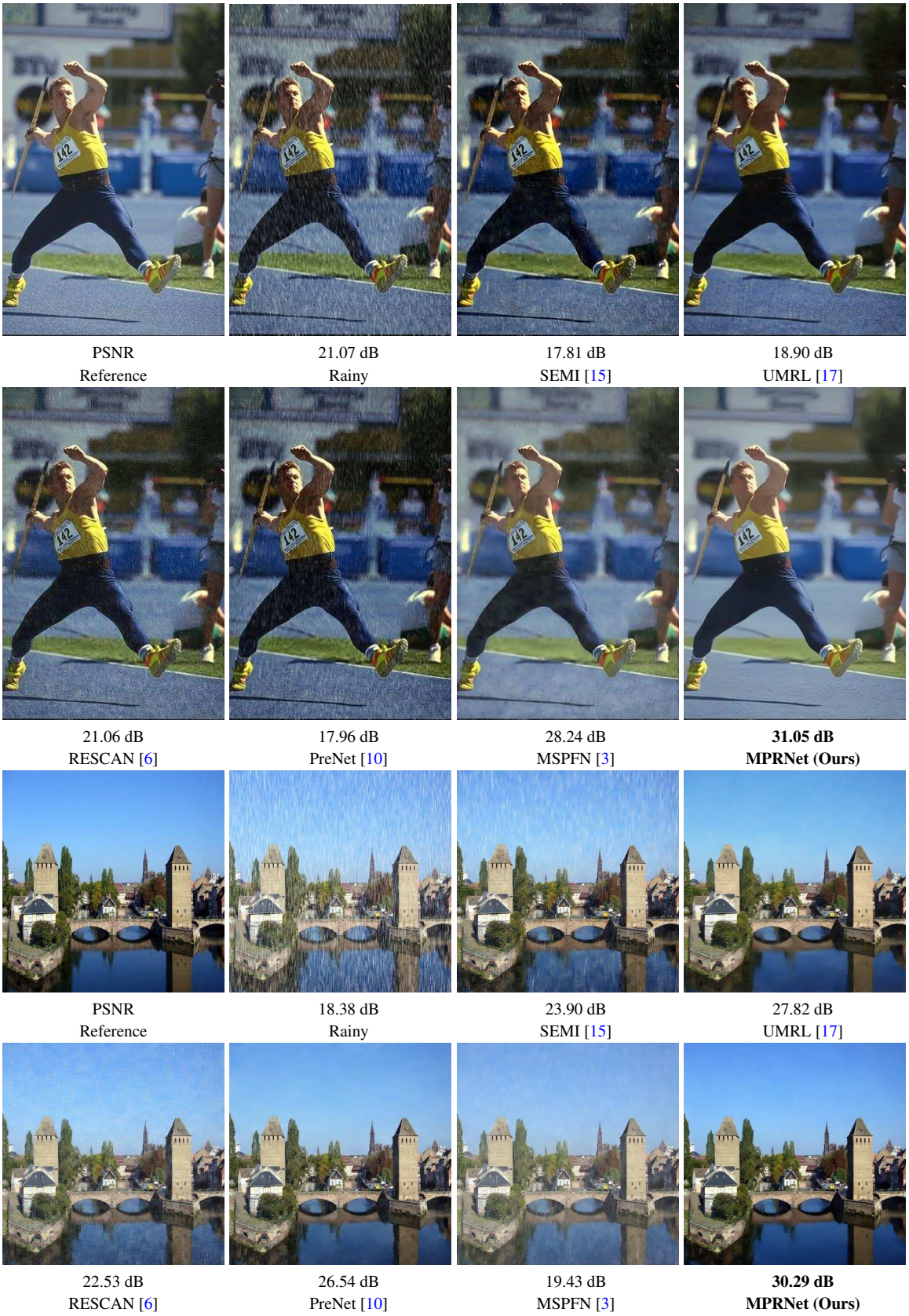

Figure 2: Visual examples for image deraining. Top image is from Test100 [22], and the bottom is from Test1200 [21].

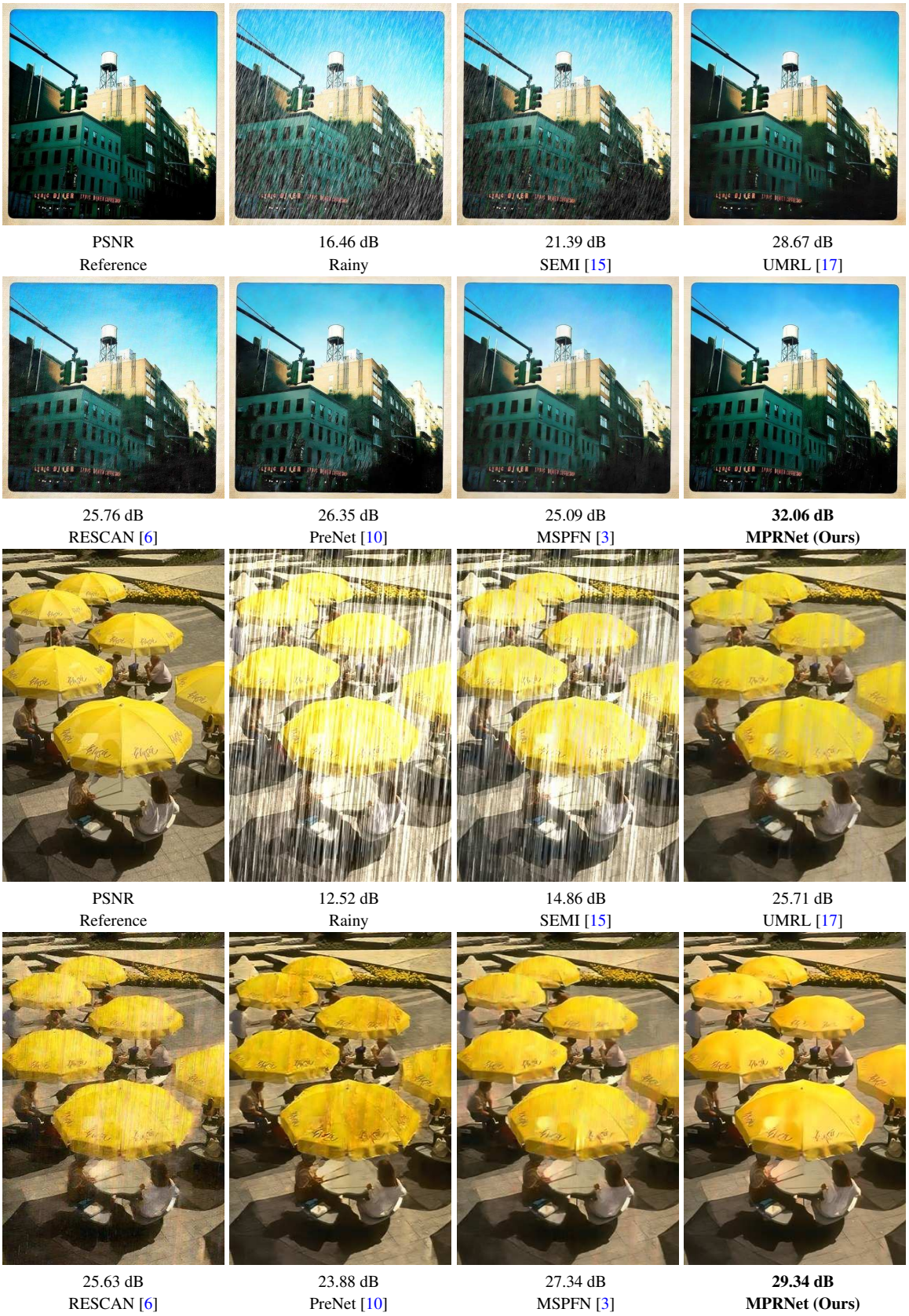

Figure 3: Visual examples for image deraining. Top image is from Test1200 [21], and the bottom is from Rain100H [16].

Figure 4: Visual examples for image deraining. Top image is from Rain100H [16], and the bottom is from Test100 [22].

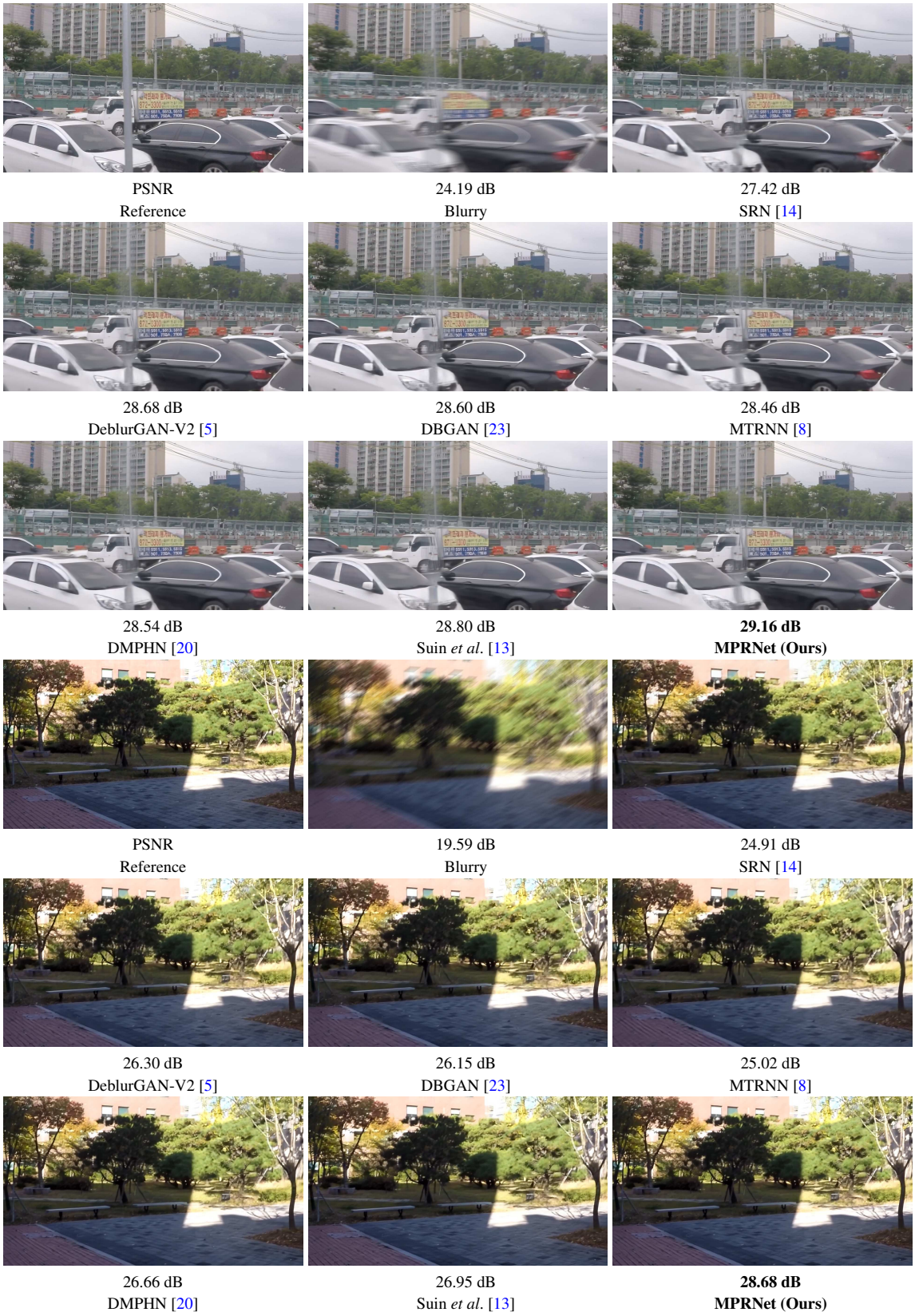

Figure 5: Image deblurring comparisons on the GoPro dataset [7]. The full-resolution versions of the images provided in Figure 6 of the main paper.

Figure 6: Image deblurring comparisons on the GoPro dataset [7].

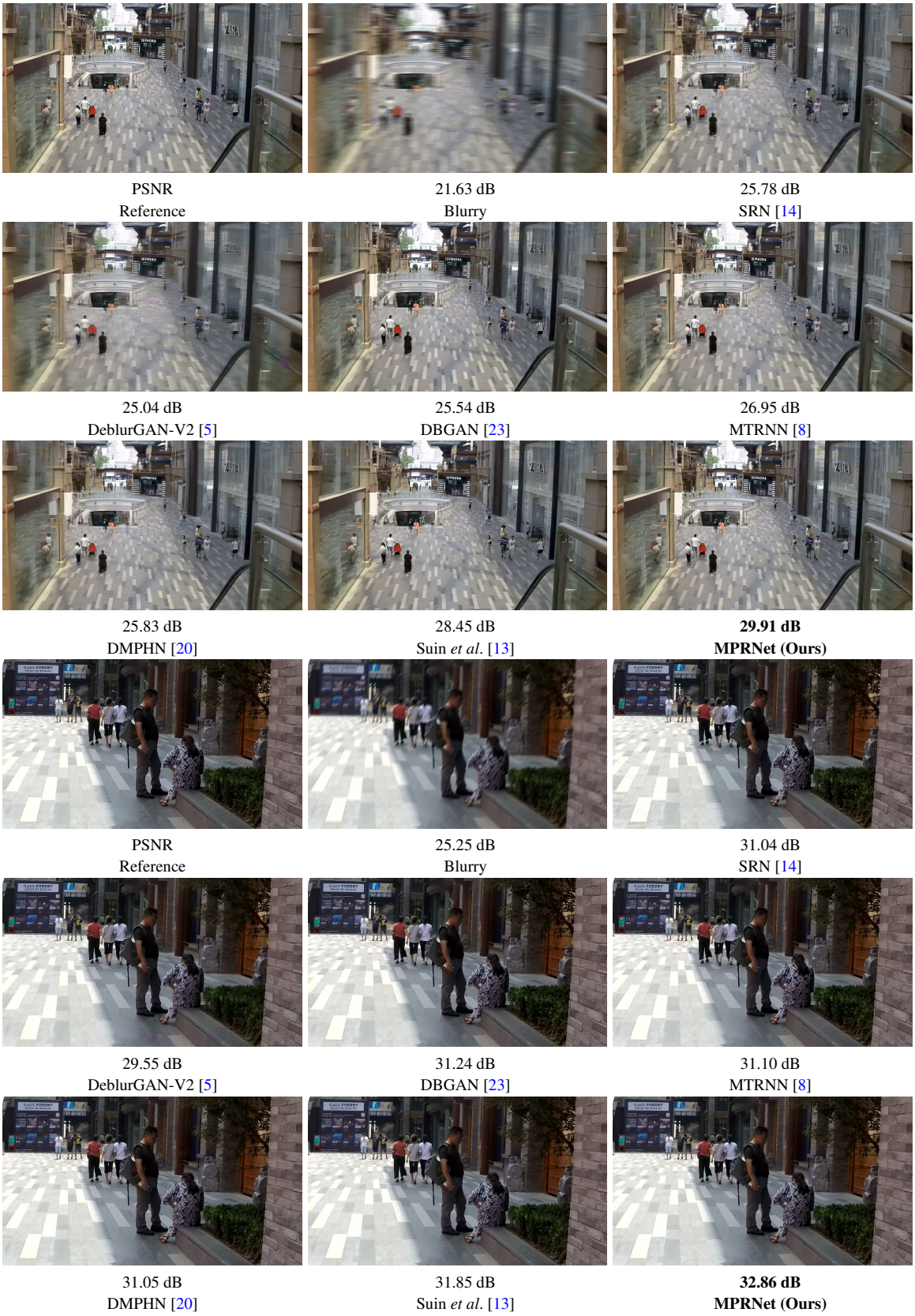

Figure 7: Image Deblurring results on the HIDE dataset [12].

Figure 8: Image Deblurring results on the HIDE dataset [12].

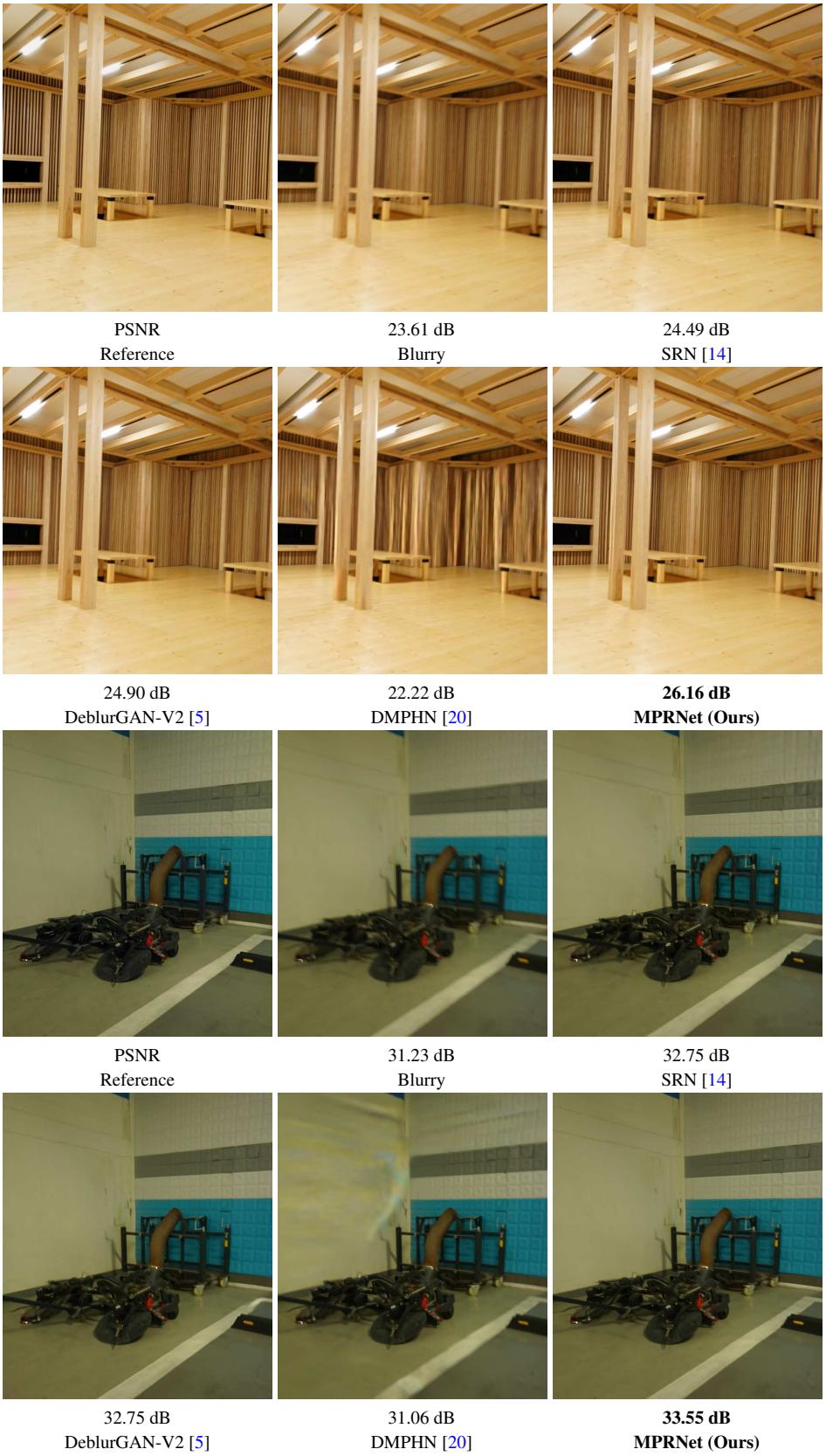

Figure 9: Image Deblurring results on RealBlur-J subset[11].

PSNR
Reference

27.08 dB
Blurry

28.94 dB
SRN [14]

28.87 dB
DeblurGAN-V2 [5]

27.72 dB
DMPHN [20]

29.31 dB
MPRNet (Ours)

PSNR
Reference

24.64 dB
Blurry

25.06 dB
SRN [14]

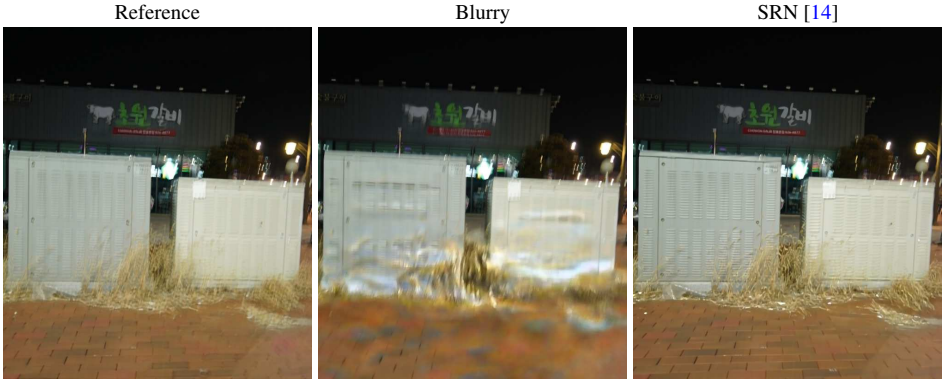

24.80 dB
DeblurGAN-V2 [5]

22.46 dB
DMPHN [20]

25.66 dB
MPRNet (Ours)

Figure 10: Image Deblurring results on RealBlur-J subset[11].

PSNR	36.82 dB	37.29 dB
Reference	Blurry	SRN [14]

37.27 dB	37.10 dB	**38.02 dB**
DeblurGAN-V2 [5]	DMPHN [20]	**MPRNet (Ours)**

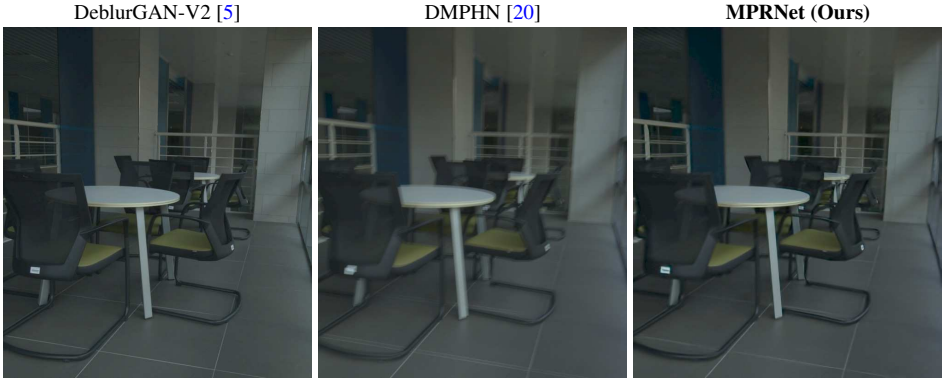

PSNR	36.54 dB	40.59 dB
Reference	Blurry	SRN [14]

37.81 dB	39.43 dB	**42.59 dB**
DeblurGAN-V2 [5]	DMPHN [20]	**MPRNet (Ours)**

Figure 11: Image Deblurring results on RealBlur-R subset[11].

PSNR
Reference

43.41 dB
Blurry

43.93 dB
SRN [14]

40.90 dB
DeblurGAN-V2 [5]

44.53 dB
DMPHN [20]

45.73 dB
MPRNet (Ours)

PSNR
Reference

41.23 dB
Blurry

40.42 dB
SRN [14]

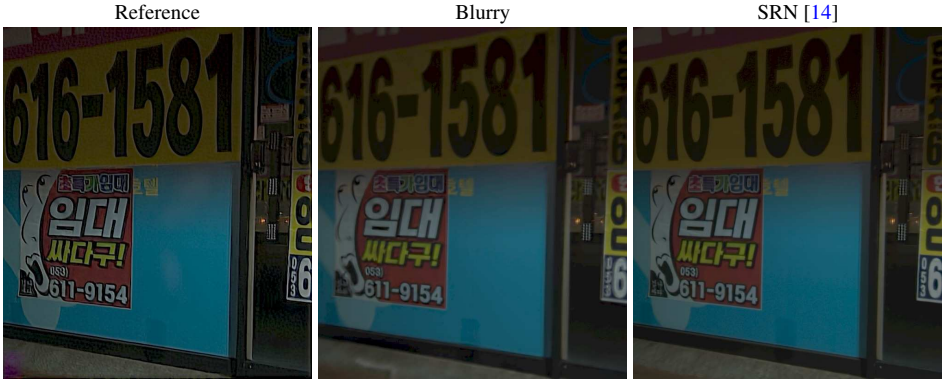

37.56 dB
DeblurGAN-V2 [5]

42.75 dB
DMPHN [20]

44.26 dB
MPRNet (Ours)

Figure 12: Image Deblurring results on RealBlur-R subset[11].

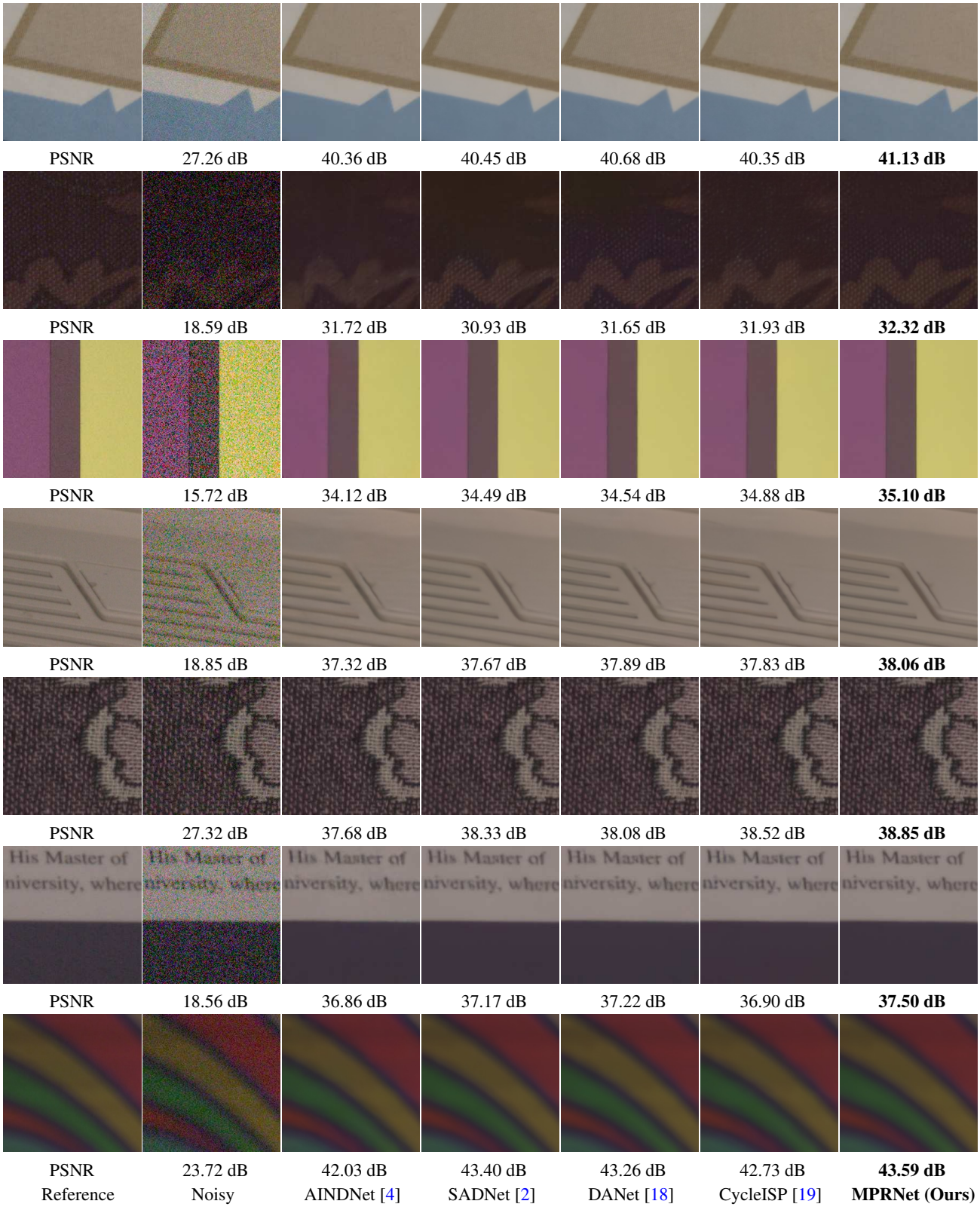

Figure 13: Denoising comparisons on the SIDD dataset [1].

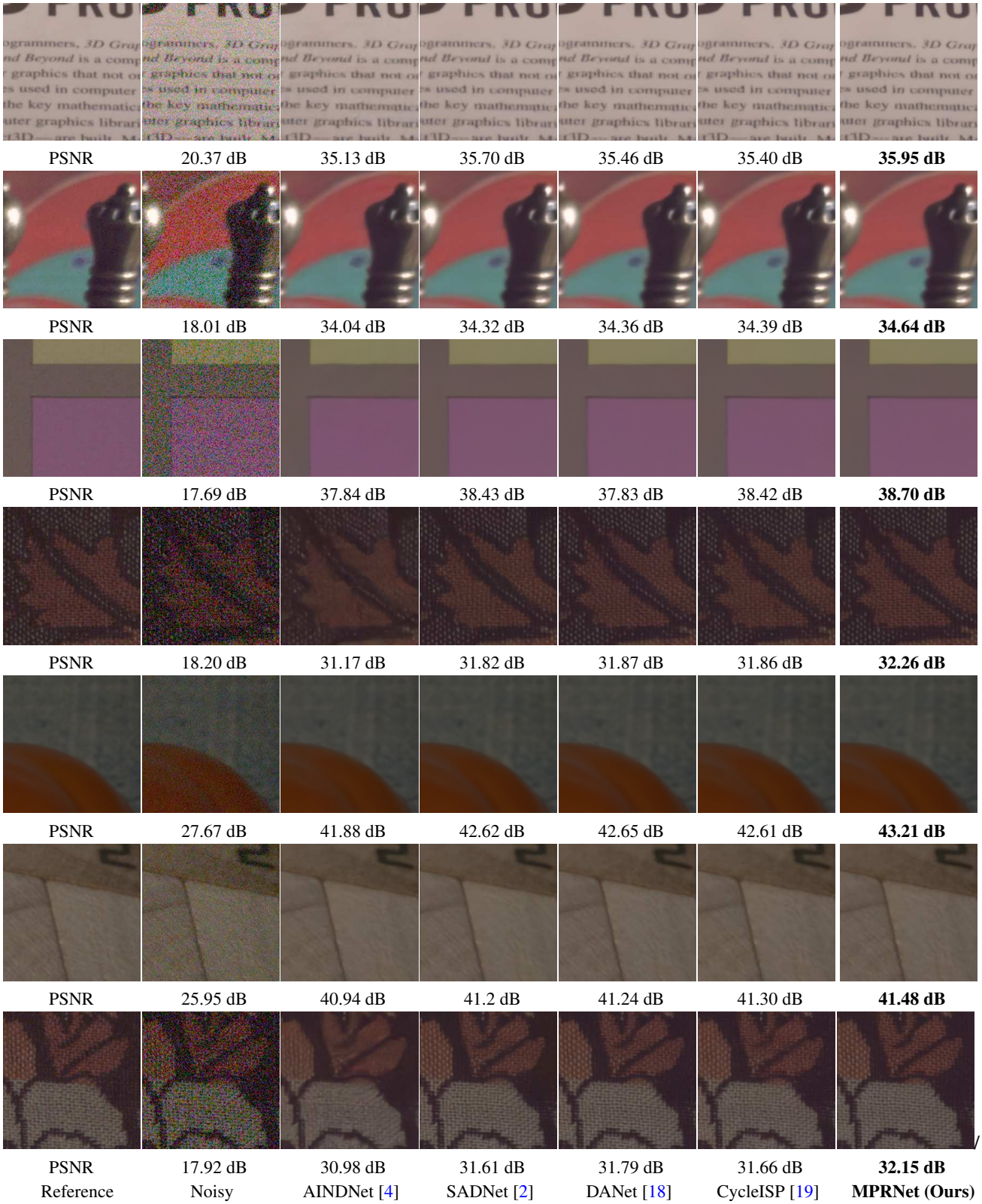

Figure 14: Denoising comparisons on the SIDD dataset [1].

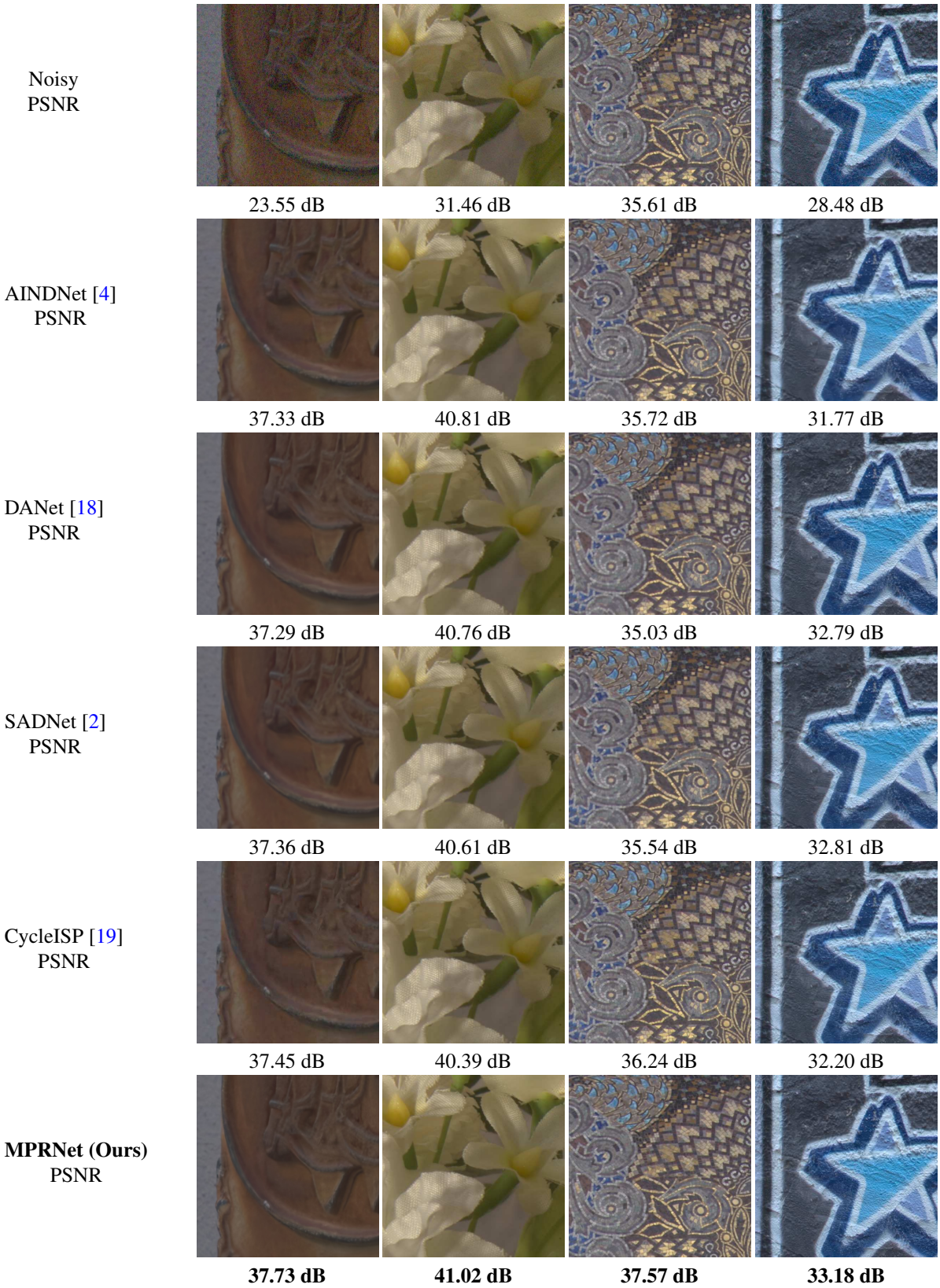

Figure 15: Denoising examples from the DND benchmark dataset [9].